A XAFS study of the local environment and reactivity of Pt- sites in functionalized UiO-67 MOFs

2016 J. Phys.: Conf. Ser. 712 012125

(http://iopscience.iop.org/1742-6596/712/1/012125)

Journal of Physics: Conference Series **712** (2016) 012125 doi:10.1088/1742-6596/712/1/012125

A XAFS study of the local environment and reactivity of Pt-sites in functionalized UiO-67 MOFs

E Borfecchia[*,1], S Øien[2], S Svelle[2], L Mino[1], L Braglia,[1,4] G Agostini[1,3], E Gallo[1,3], K A Lomachenko[1,4], S Bordiga[1], A A Guda[4], M A Soldatov[4], A V Soldatov[4], U Olsbye[2], K P Lillerud[2], C Lamberti[4,5]

[1]Dept. of Chemistry, NIS and INSTM Reference Centers, University of Turin, Turin (Italy);
[2]inGAP Centre for Research Based Innovation, Dept. of Chemistry, University of Oslo, Oslo (Norway);
[3]European Synchrotron Radiation Facility (ESRF), Grenoble (France);
[4]Southern Federal University, Rostov-on-Don (Russia);
[5]Dept. of Chemistry, CrisDi Centre for Crystallography, University of Turin, Turin (Italy)

E-mail: elisa.borfecchia@unito.it

Abstract. We synthesized UiO-67 Metal Organic Frameworks (MOFs) functionalized with bpydcPt(II)Cl_2 and bpydcPt(IV)Cl_4 complexes (bpydc = bipyridine-dicarboxylate), as attractive candidates for the heterogenization of homogeneous catalytic reactions. Pt L_3-edge XAFS experiments allowed us to thoroughly characterize these materials, in the local environment of the Pt centers. XAFS studies evidenced the rich reactivity of UiO-67-Pt(II) MOFs, including reduction to bpydcPt(0) under H_2 flow in the 600−700 K range, room-temperature oxidation to bpydcPt(IV)Br_4 through oxidative addition of liquid Br_2 and ligand exchange between 2 Cl^- and even bulky ligands such as toluene-3,4-dithiol. Preliminary XANES simulations with ADF code provide additional information on the oxidation state of Pt sites.

1. Introduction

Metal-organic frameworks (MOFs) are crystalline, porous solids consisting of metal ions or clusters, coordinated with organic linkers [1]. The recently discovered UiO-66 and UiO-67 classes of iso-structural MOFs are obtained connecting $Zr_6O_4(OH)_4$ inorganic cornerstones with 1,4-benzene-dicarboxylate or 4,4′ biphenyl-dicarboxylate linkers, for the UiO-66 and UiO-67 MOFs, respectively [2]. Due to their outstanding stability at high temperatures, high pressures and in presence of different solvents, these materials are among the few MOFs already commercialized for applications in the fields of catalysis, H_2 storage, and gas purification [1,2]. We are currently exploring the possibility to enhance the capabilities of the UiO-67 MOF by grafting to the framework an additional catalytically-active Pt center, by chelating bipyridine-dicarboxylate (bpydc) linkers [3]. The resulting metal-functionalized MOFs are attractive candidates for industrial applications aiming to heterogenization of homogeneous catalytic reactions. Due to the local character of the functionalization process, XAFS has played a key role in clarifying the local structural and electronic properties of the grafted metal center [4, 5].

2. Experimental

Pt-functionalized UiO-67 materials, hereafter UiO-67-Pt(II) and UiO-67-Pt(IV), were synthesized by the standard solvothermal method, by reacting $ZrCl_4$ with a mixture of H_2bpdc and (H_2bpydc)/$PtCl_x$(H_2bpydc) (x = 2 or 4; the ratio between the linkers being 9:1, and equal molar quantity of $ZrCl_4$ and linker) in a solution of DMF [3].

Pt L_3-edge (11564 eV) XAFS data were collected at the I811 beamline @ Max Lab II (Lund, Sweden). The white beam produced by a liquid He-cooled superconducting wiggler was monochromatized by an horizontally sagitally focused double-crystal Si(111) monochromator, detuned to 20% to minimize the third harmonic. Spectra were collected in transmission mode using 30 cm ionization chambers for I_0 and I_1 and by a photodiode for I_2. MOF samples were measured inside a home-made cell allowing sample activation and gas dosage under *in situ* or *operando* conditions [6]. The EXAFS spectra were extracted and analyzed with Athena and Arthemis codes [7]. Geometry relaxation, electronic structure and Pt L_3 XANES calculations were performed by means of molecular orbital density functional theory implemented in ADF-2014 software [8]. B3LYP exchange correlation functional and large QZ4P basis set were used in all simulations.

3. Results and discussion

In this contribution we present results on UiO-67 functionalized with bpydcPt(II)Cl_2 and bpydcPt(IV)Cl_4 coordination complexes acting as linkers in the MOF framework and prepared following three different synthesis methods: (i) one-pot synthesis (OPS) where $ZrCl_4$ and $PtCl_x$ (x = 2 or 4) precursors salts react with biphenyl and bipyridine linkers; (ii) premade linker synthesis (PMLS), where a previously prepared $PtCl_x$(H_2bpydc) linker reacts with biphenyl linkers and $ZrCl_4$; and (iii) post-synthesis functionalization (PSF), where a premade UiO-67-bpy MOF is suspended in a solution of precursor $PtCl_x$ salt [3].

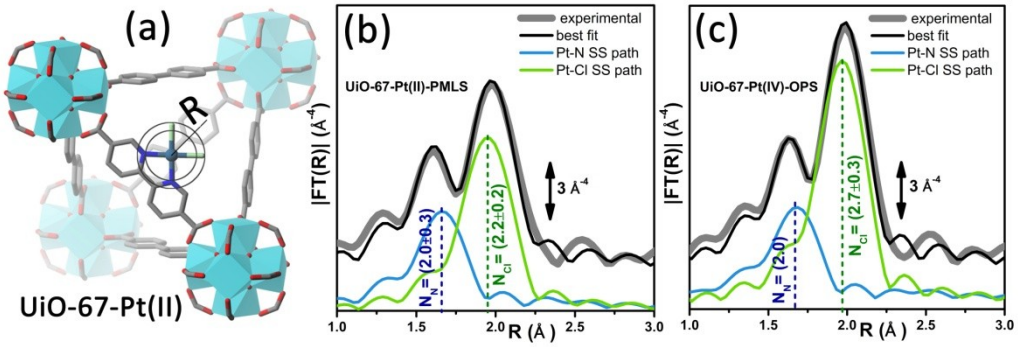

Figure 1. (a) Three-dimensional representation of UiO-67-Pt(II) MOF, evidencing the structure of the isolated H_2bpydc$PtCl_2$ center inserted in the MOF structure, with 2 N and 2 Cl in the first coordination shell of Pt(II) (atoms color code: Pt: dark cyan, N: blue, Cl: light green, C: gray, O: red, Zr cornerstones: light cyan). (b,c) Experimental FT of the k^3-weighted EXAFS spectra collected for a typical (b) UiO-67-Pt(II) sample (PMLS synthesis) and (c) UiO-67-Pt(IV) sample (OPS synthesis) and their corresponding best fits; moduli of Pt−N and Pt−Cl single scattering paths are also reported, vertically shifted for the sake of clarity, together with the respective coordination numbers refined in the EXAFS fit.

With the only exception of the UiO-67-Pt(II)-OPS, that crystallizes together with a fraction of about 40% of amorphous (nonporous) phase, the remaining syntheses resulted in high crystalline materials with porosity close to the target ideal structure. XRPD and Pt L_3-edge XAFS studies proved that the three synthesis methods are equivalent and for Pt(II) samples fully comply with the target structure (figure 1a) on both long-range (ordered MOF framework) and short-range (local environment of Pt sites probed by XAFS) scales. The last point has also been supported by Pt L_3 valence-to-core RIXS maps [3]. XAFS also revealed that the incorporation of Pt(IV) sites into the UiO-67 MOF is more critical. Although the synthesis of stable Pt(IV) linkers was successful (see figure 3a for XANES

spectra of H_2bpydcPtCl_2 and H_2bpydcPtCl_4 linkers), during the preparation of the UiO-67-Pt(IV) MOFs a significant fraction of bpydcPt(IV)Cl_4 sites is reduced to bpydcPt(II)Cl_2, resulting in a final average Pt-coordination number $N_{Cl} = (2.7 \pm 0.3)$, lower than the target value $N_{Cl} = 4$ (figure 1c).

UiO-67-Pt(II) systems were further tested toward accessibility and reactivity to molecules of small- (e.g. H_2), medium- (e.g. Br_2), and large-size (e.g. thiol), resulting in the reactive paths represented in figure 2. H_2-temperature programmed reduction (TPR) treatments have been followed under *operando* conditions by Pt L_3-edge EXAFS, showing that Cl ligands can be selectively removed as HCl molecules in the 600−700 K temperature range, resulting in bpydcPt(0) complexes linked to the MOF framework (reduction path, figure 2a). This result was derived from a sophisticated parametric analysis of the H_2-TPR datasets (figure 2b), where all the EXAFS spectra collected in the 300−750 K range have been simultaneously refined, adopting the Einstein model for the Pt−N and Pt−Cl Debye-Waller factors [3]. These findings were also supported by FTIR spectroscopy, which evidences the high coordinative unsaturation of the reduced Pt centers, able to form a variety of Pt monocarbonyl complexes and also bpydcPt(0)$(CO)_2$ dicarbonyl complexes upon CO adsorption. The formation of EXAFS-silent Pt(0)-hydrogen species in these conditions is currently under investigation, as well as the effect of higher H_2 concentration during H_2-TPR, possibly inducing aggregation of the isolated Pt(0) sites into highly reactive metal nanoclusters.

The large pore size of UiO-67 allows for ligand exchange between 2 Cl^- and even bulky ligands such as toluene-3,4-dithiol (H_2tdt, ligand exchange path, figure 2c). Framework bpydcPt(II)Cl_2 complexes can also be oxidized at room temperature to bpydcPt(IV)Br_4 through oxidative addition of liquid Br_2 (oxidation path, figure 2d). With this respect, EXAFS monitored the ligand exchange in the first coordination shell of Pt (figure 2), while XANES spectroscopy was used to monitor the changes in the Pt oxidation state along the observed reactions (figure 3).

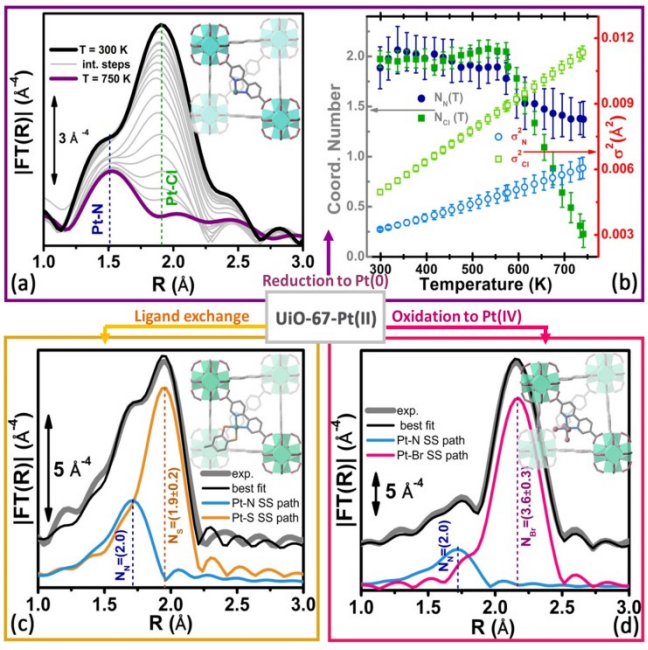

Figure 2. Reactivity of Pt(II) species in functionalized UiO-67-Pt MOFs as evidenced by EXAFS in *operando* and static conditions. (a,b) Reduction path: (a) FT of the k^3-weighted Pt L_3-edge EXAFS spectra collected during *operando* H_2-TPR experiments on UiO-67-Pt(II)_PMLS MOFs, simultaneously refined adopting the Einstein model for the Pt−N and Pt−Cl Debye-Waller factors, as shown in part (b). (c,d) Experimental FT of the k^3-weighted Pt L_3-edge EXAFS spectra and corresponding best fit curves for UiO-67-Pt(II) after interaction with (c) H_2tdt (ligand exchange path) and (d) Br_2 (oxidation path). Single scattering contributions to first shell EXAFS signal in the two cases (Pt−N and Pt−S in part (c) and Pt−N and Pt−Br in part (d)) are also reported, vertically shifted for the sake of clarity, with indicated the correspondent coordination numbers refined in the fit.

Simulated XANES spectra, calculated with ADF code (figure 3b,d), were able to reproduce correctly the variation of the white line intensity for UiO-67-Pt(II) and -Pt(IV) linkers (figure 3a), and UiO-67-Pt(II) MOF before and after the interaction with H_2tdt and Br_2 (figure 3c). Indeed, white line intensity in L_3-edge XANES is directly proportional to the density of the unoccupied 5d states and consequently it provides information on the formal charge (or valence) of Pt species [3]. In particular, XANES simulations confirmed that after ligand exchange with H_2tdt the pristine Pt(II) oxidation state

is conserved, whereas interaction with Br_2 results in oxidized H_2bpydcPt(IV)Br_4 complexes. In a successive work, we plan to use the ADF calculated unoccupied molecular orbitals for improving the simulation of the XANES spectra in dipole one-electron approximation along with finite difference method with an upgraded version of the FDMNES code [9].

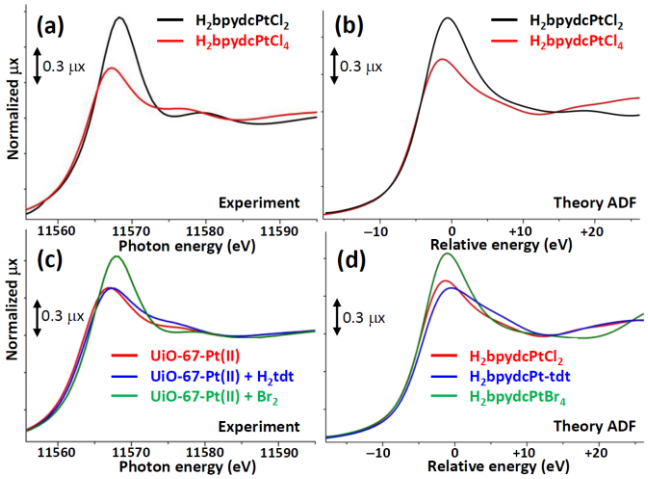

Figure 3. (a) Experimental XANES spectra of the H_2bpydcPtCl_2 and H_2bpydcPtCl_4 linkers. (b) Corresponding theoretical spectra computed with ADF code. (c) Experimental XANES spectra of UiO-67-Pt(II) MOF before (red curve) and after interaction from the liquid phase with H_2tdt and Br_2. (d) Theoretical spectra computed with ADF code of the H_2bpydcPtCl_2, H_2bpydcPt(tdt) and H_2bpydcPtBr_4 molecular fragments.

In conclusion, XAFS allowed us to thoroughly characterize the local coordination environment and oxidation states in a series of Pt(II)- and Pt(IV)-functionalized UiO-67 MOFs, synthesized by different methods. By combing EXAFS in static and *operando* conditions with DFT-assisted XANES simulations we also explored the rich reactivity of Pt(II) sites, undergoing reduction, oxidation and ligand exchange reactions. These results pave the way to further studies aiming to assess the performance of these systems for the heterogenization of specific homogeneous catalytic reactions.

Acknowledgments
C L, K A L, A A G and A V S acknowledge the megagrant of the Russian Federation Government to support scientific research at the Southern Federal University, no. 14.Y26.31.0001.

References

[1] Ferey G 2008 *Chem. Soc. Rev*. **37** 191; Long J.R and Yaghi O M 2009 *Chem. Soc. Rev*. **38** 1213; Bordiga S, Bonino F, Lillerud K-P and Lamberti C 2010 *Chem. Soc. Rev*. **39** 4885; Butova V V, Soldatov M A, Guda A A, Lomachenko K A and Lamberti C, 2016 *Russ. Chem. Rev*., **85** doi:10.1070/RCR4554.

[2] Cavka J H, Jakobsen S, Olsbye U, Guillou N, Lamberti C, Bordiga S, Lillerud K-P 2008 *J. Am. Chem. Soc*. **130** 13850; Valenzano L, Civalleri B, Chavan S, Bordiga S, Nilsen M H, Jakobsen S, Lillerud K-P, Lamberti C. 2011 *Chem. Mater*. **23** 1700; Chavan S, Vitillo J G, Gianolio D, Zavorotynska O, Civalleri B, Jakobsen S, Nilsen M H, Valenzano L, Lamberti C, Lillerud K-P, Bordiga S. 2012 *Phys. Chem. Chem. Phys*. **14** 1614.

[3] Øien S, Agostini G, Svelle S, Borfecchia E, Lomachenko K A, Mino L, Gallo E, Bordiga S, Olsbye U, Lillerud K-P and Lamberti C 2015 *Chem. Mater*. **27** 1042.

[4] Bordiga S, Groppo E, Agostini G, van Bokhoven J A and Lamberti C. 2013 *Chem. Rev*. **113** 1736; Mino L, Agostini G, Borfecchia E, Gianolio D, Piovano A, Gallo E and Lamberti C. 2013 *J. Phys. D: Appl. Phys*. **46** 423001; Garino C, Borfecchia E, Gobetto R, van Bokhoven J A and Lamberti C. 2014 *Coord. Chem. Rev*. **277–278** 130.

[5] van Bokhoven J A, and Lamberti C, 2016 *X-Ray Absorption and X-ray Emission Spectroscopy: Theory and Applications*, Eds. Vol. 1,2 (Chichester: John Wiley & Sons).

[6] Lamberti C, Prestipino C, Bordiga S, Berlier G, et al. 2003 *Nucl. Instr. Meth. B,* **200** 196.

[7] Ravel B and Newville M 2005 *J. Synchrotron Radiat*. **12** 537.

[8] Fonseca Guerra C, Snijders J G, te Velde G, Baerends E J, 1998 *Theor. Chem. Acc*. **99**, 391; te Velde, G, Bickelhaupt F M, Baerends E J, Guerra C F, et al. 2001 *Comput. Chem*. **22** 931.

[9] Guda S A, Guda A A, Soldatov M A, Lomachenko K A, Bugaev A L, Lamberti C, Gawelda W, Bressler C, Smolentsev G, Soldatov A V, Joly Y, 2015 *J. Chem. Theory Comput.* **11** 4512.; *J. Phys.: Conf. Ser*., these proceedings.